



## A NOVEL ILLUMINATION CORRECTION AND INTENSITY NORMALIZATION METHOD ON CERVIGRAMS IN THE EARLY DETECTION OF UTERINE CERVICAL CANCER

Abhishek Das<sup>1</sup>, Avijit Kar<sup>2</sup> and Debasis Bhattacharyya<sup>3</sup>

<sup>1</sup>Department of Information Technology, Tripura University (A Central University), Agartala, India

<sup>2</sup>Department of Computer Sc. & Engineering, Jadavpur University, Kolkata, India

<sup>3</sup>Department of Gynecology, College of Medicine & Sagore Dutta Hospital, Kolkata, India

E-Mail: [adas@tripurauniv.in](mailto:adas@tripurauniv.in)

### ABSTRACT

Cervical Cancer is one of the ubiquitous forms of cancer afflicting the female population worldwide. A Colposcope is a self-illuminated microscope which acquires the image of the affected cervix and the image is known as a cervigram. The raw cervigram is preprocessed by removing the specular reflections and then the region of interest is sought. Before the image is made ready for implementing further image processing algorithms, our novel illumination correction and intensity normalization methods are applied. In the current paper we propose a novel method where we use the polynomial-type Newton's divided difference interpolation for illumination correction. Based on our research findings, we conclude that the peak of the entire cervix region intensity distribution is strongly correlated with the peak of the SE region intensity distribution.

**Keywords:** cervical cancer, normalization, illumination correction.

### INTRODUCTION

Uterine Cervical Cancer is one of the ubiquitous forms of cancer afflicting the female population worldwide. According to WHO [1], [2], every year in India alone there are 1 lakh 30 thousand women who are affected with cervical cancer. According to Chittaranjan National Cancer Research Institute's Cancer Registry Program [3], [4], in the state of West Bengal alone, out of every 1000 women, aged between 30 years to 60 years old, 18 are affected by cervical cancer. The real numbers of affected cervical cancer patients are still unknown, as the state has in-adequate infrastructure. With lack of awareness and treatment, the deadly disease gets detected only in the Cancer Final Stage. Due to cervical cancer alone, 80,000 women dies every year in our Country [5],[6],[7],[8]. A Colposcope is a self-illuminated microscope which acquires the image of the affected cervix and the image is known as a cervigram. The raw cervigram is preprocessed by removing the specular reflections and then the region of interest is sought. Before the image is made ready for implementing further image processing algorithms, illumination correction methods and intensity normalization methods are applied.

### LITERATURE REVIEW

The Region of Interest (ROI) extracted in the pre-processing step is gross and often includes extended parts of the vaginal region [9],[10]. Numerous segmentation methods [11],[12] can be used to refine the detection quality of the cervix boundary. These include region-growing and energy minimization functional. In region growing [13] a region is defined via propagation of similar neighboring pixels. A region-growing scenario in the cervix boundary detection task can be defined as spreading the region from a solo point located in the center of the initial ROI. The choice of acceptable features for the

propagation is not a trivial task, as different images will require a different set of features in order to advance the region from the center of the cervix to its boundaries. The region-growing can be thrown to disorder by other tissues within the cervix [4],[2]. The boundaries procreated in this way cannot be restricted by any smoothing or shape continece [14].

Segmentation that combines edge and region information can be accomplished using an energy minimization technique via the active contour edifice. The edifice can be sub classified into snakes [15] and level set [16] methods, two different schemes to carry out the contour deformation process. A review and comparison between different energy functional was recently presented [17]. A main inference of the review, in which both methods were evaluated on a set of different medical images, was that the integration of forces from different energy functional may lead to better segmentation results. The main whip hand of such methods, as compared to region growing, is their ability to integrate local and global information and to account for both region and edge features, while preserving smoothness of the boundaries [18].

### Our Proposed method

In the current article energy minimization via active contours is used in order to refine the initial ROI so that it matches the actual cervix boundaries more closely. The main contribution of the current work is the energy functional used, that consists of forces and features adequate for the task of cervix boundary detection. Region edge, and prior shape information [19],[20] are all used for this objective. We use the implicit implementation via level-sets. Implementation via the parametric snake mechanism may be possible a well.



In an active contour framework the image is considered as a function  $I : \Omega \rightarrow \mathbb{R}^+$  where  $\Omega \in \mathbb{R}^2$  is the image domain. The segmentation problem is mathematically formulated as the search for a contour  $C : [0, L] \rightarrow \mathbb{R}^2$  in the image, which is optimal with respect to some pre-defined integral measure,  $E(C)$ , also called the energy functional. Formally, this problem is stated as:

$$C = \arg \min_C E(C).$$

In the current work the energy functional consists of two terms: a data term and a shape prior term:

$$E(C) = E_{\text{data}}(C) + \alpha E_{\text{shape}}(C)$$

The data term is activated first and evolves the curve according to features derived from the input image. The shape term is added next and better aligns the contour to a predefined model of the cervix shape. The  $\alpha$  parameter is a time dependent parameter that controls the activation sequence of the two terms.

### Our proposed Illumination Correction method

A benchmark method for illumination correction [21],[22] is to estimate the illumination field as a single model derived from the lighting conditions and the shape of the object [13]. Lighting conditions can be computed from a training set of images with known intensity values under ordinary lighting [23]. Shading artifacts generated due to the three-dimensional shape of an object can be corrected using Lambert's cosine law when lighting conditions are known [24]. Various other works iterate a per-image illumination correction, among them Retinex algorithm for image enhancement [28], [29], which provides a strong dynamic range compression and color consistency [30] and is based on the hypothesis that the illumination field is spatially smooth.

In the current article, the illumination correction method is based on the assumption that the cervix content can be modeled by a mixture of Gaussians. A per-image illumination field correction is performed based on this assumption and iterations combining segmentation with illumination field estimation. The algorithm extant here is based on the expectation maximization algorithm (EM) [31] for bias correction in MR images of the brain.

A description of the EM application to cervigrams is provided as follows: Cervigram tissues are described in the CIE- Lab color space. The illumination correction process is applied to the L channel which represents the intensity levels of each pixel and is the only channel influenced from illumination changes [13]. The adjacent channels a and b remain unaffected. The L channel is initially down-sampled, which debilitatingly improves the results while substantially reducing the running time. As the illumination field is considered to be multiplicative [13], a logarithmic transformation is performed on the L channel in order to make it additive and to simplify the computations. The illumination changes gradually within the image plane, thus it can be modeled by a polynomial. A polynomial-type Lagrange interpolation was proposed by [32] and 2d Lagrange's interpolation basis functions were proposed [33]. In the

current work we use the polynomial-type Newton's divided difference interpolation. The following interpolation is used:  $I = \sum_{k=1}^K c_k \phi_k(x)$ , where  $c_k$  are the illumination field parameters,  $\phi_k$  are Newton's divided difference interpolation basis functions and  $K$  is the number of the interpolation points. The interpolation points are located on an equally spaced grid of the image size with  $N \times N = K$  points at positions  $(x, y)$  of the image spatial coordinates.

The Newton's divided difference quadratic polynomial interpolation- formula is given as follows:

Given  $(x_0, y_0)$ ,  $(x_1, y_1)$  and  $(x_2, y_2)$ , fit a quadratic interpolant through the data. Noting  $y=f(x)$ ,  $y_0=f(x_0)$ ,  $y_1=f(x_1)$  and  $y_2=f(x_2)$ , assume the quadratic interpolant  $f_2(x)$  is given by

$$f_2(x) = b_0 + b_1(x - x_0) + b_2(x - x_0)(x - x_1)$$

At  $x = x_0$ ,

$$f_2(x_0) = b_0 + b_1(x_0 - x_0) + b_2(x_0 - x_0)(x_0 - x_1) = b_0$$

$$b_0 = f(x_0)$$

At  $x = x_1$ ,

$$f_2(x_1) = f(x_1) = b_0 + b_1(x_1 - x_0) + b_2(x_1 - x_0)(x_1 - x_1)$$

$$f(x_1) = f(x_0) + b_1(x_1 - x_0)$$

Giving

$$b_1 = (f(x_1) - f(x_0)) / (x_1 - x_0)$$

At  $x = x_2$

$$f_2(x_2) = f(x_2) = b_0 + b_1(x_2 - x_0) + b_2(x_2 - x_0)(x_2 - x_1)$$

$$f(x_2) = f(x_0) + ((f(x_1) - f(x_0)) / (x_1 - x_0)) * (x_2 - x_0) + b_2(x_2 - x_0)(x_2 - x_1)$$

Giving

$$b_2 = (((f(x_2) - f(x_1)) / (x_2 - x_1)) - ((f(x_1) - f(x_0)) / (x_1 - x_0))) / (x_2 - x_0)$$

Hence the quadratic interpolant is given by

$$f_2(x) = b_0 + b_1(x - x_0) + b_2(x - x_0)(x - x_1)$$

$$= f(x_0) + ((f(x_1) - f(x_0)) / (x_1 - x_0)) * (x - x_0) + (((f(x_2) - f(x_1)) / (x_2 - x_1)) - ((f(x_1) - f(x_0)) / (x_1 - x_0))) / (x_2 - x_0) * (x - x_0)(x - x_1)$$

This leads us to writing the general form of the Newton's divided difference polynomial for  $n+1$  data points,  $(x_0, y_0)$ ,  $(x_1, y_1)$ , ...,  $(x_{n-1}, y_{n-1})$ ,  $(x_n, y_n)$ , as

$$f_n(x) = b_0 + b_1(x - x_0) + \dots + b_n(x - x_0)(x - x_1) \dots (x - x_{n-1})$$

Where

$$b_0 = f[x_0]$$

$$b_1 = f[x_1, x_0]$$

$$b_2 = f[x_2, x_1, x_0]$$

:

$$b_{n-1} = f[x_{n-1}, x_{n-2}, \dots, x_0]$$

$$b_n = f[x_n, x_{n-1}, \dots, x_0]$$



where the definition of the mth divided difference is

$$b_m = f[x_m, \dots, x_0] \\ = (f[x_m, \dots, x_1] - f[x_{m-1}, \dots, x_0]) / (x_m - x_0)$$

From the above definition, it can be observed that the divided differences are calculated recursively.

Using this model, the illumination field can be obliterated from each pixel in the image. Once the illumination field influence is removed from the intensity values, the cervix tissue can be modeled as a mixture of Gaussians in 1-d feature space. The probability of occurrence of each Gaussian  $j$  is denoted  $\alpha_j$ . For a set of  $n$  feature vectors:  $\hat{y}_1, \dots, \hat{y}_n$ , the maximum likelihood estimate of the different parameters can be found by maximizing  $f(\hat{y} | \theta, c) = \prod f(\hat{y}_i | \theta, c)$ , using the EM algorithm [25],[27],[34].

Since we have the estimate of the parameter set, each iteration of the EM algorithm re-estimates the parameter set according to the following steps:

#### ■ Expectation step

$$p(T_i = j | \hat{y}_i, \theta, c) = \frac{\alpha_j f(\hat{y}_i | \theta_j, c)}{\sum_{t=1}^J \alpha_t f(\hat{y}_i | \theta_t, c)}$$

#### ■ Maximization step of the Mixture of Gaussian parameters:

$$\alpha_j = \frac{\sum_i p(T_i = j | \hat{y}_i, \theta, c)}{n}, \\ \mu_j = \frac{\sum_i p(T_i = j | \hat{y}_i, \theta, c)(y_i - \sum_k c_k \phi_k(x_i))}{\sum_i p(T_i = j | \hat{y}_i, \theta, c)}, \\ \sigma_j^2 = \frac{\sum_i p(T_i = j | \hat{y}_i, \theta, c)(y_i - \sum_k c_k \phi_k(x_i) - \mu_j)^2}{\sum_i p(T_i = j | \hat{y}_i, \theta, c)}$$

#### ■ Maximization step of the illumination field parameters:

$$\begin{bmatrix} c_1 \\ c_2 \\ \vdots \\ c_K \end{bmatrix} = (A^T W A)^{-1} A^T W R; \quad A = \begin{bmatrix} \phi_1(x_1) & \phi_2(x_1) & \dots & \phi_K(x_1) \\ \phi_1(x_2) & \phi_2(x_2) & \dots & \phi_K(x_2) \\ \vdots & \vdots & \dots & \vdots \end{bmatrix} \\ W = \text{diag}(w_i); \quad w_i = \sum_j w_{ij}; \quad w_{ij} = \frac{p(T_i = j | \hat{y}_i, \theta, c)}{\sigma_j^2}$$

$$R = \begin{bmatrix} y_1 - \bar{y}_1 \\ y_2 - \bar{y}_2 \\ \vdots \end{bmatrix}; \quad \bar{y}_i = \frac{\sum_j w_{ij} \mu_j}{\sum_j w_{ij}}$$

Where  $T_i$  is the tissue type at position  $I$ ,  $A$  is the interpolation matrix representing the geometry of the illumination field,  $W$  is the diagonal matrix holding the sum over all weights,  $w_{ij}$ , assigned to each pixel. The predicted pixel intensity value is  $y_i$ , and  $R$  is a vector that represents a rough estimation of the illumination-field at every pixel. As the EM algorithm gets worked on the cervigrams, several concerns need to be addressed:

The degree of the polynomial that estimates the illumination field needs to be set. It defines the smoothness of the illumination field and has a strong influence on the quality of the residual signal within the L channel. If due to a large polynomial degree, the surface is not suave enough, vital information that relates to the different tissues within the cervix might be missing, leading to a poor comparison between them. It was observed that the surface of the illumination field is best elaborated as a sixth degree polynomial ( $K = 38$  interpolation points).

When the EM algorithm is applied in MR brain images [31] for bias correction, an a-priori anatomical atlas of the brain is used in order to initialize the Mixture of Gaussian parameters. But for the cervigram images, no such atlas is acquirable, a standard K-means clustering algorithm is used to estimate the initial values of mean and standard deviation.

The cervix region is occupied by the SE, CE and AW tissues and an additional group for the remaining tissues, thus amounting to total number of tissues  $J=4$ . The illumination field estimation should not depend to this number as pixels that possess significantly different intensity values from any of the Gaussian distributions with low  $w_{ij}$  values and they must be having little influence on the illumination field estimation.

#### Intensity Normalization method

Due to different image acquisition techniques of cervigrams, as with health workers in different light conditions, a large diversity of intensity range exist within the cervigram image database. In order to learn global tissue models in a supervised manner and to compare images across the data-set, a dynamic range normalization step is essential. A cervigram specific normalization procedure is therefore proposed. The hypothesis is based on the fact that the squamous epithelium (SE) tissue should have a similar dynamic range of intensities across the image set, as it is the original cervix tissue. The hypothesis is based on the following set of observations drawn from a set of 200 manually marked cervigrams. The SE tissue is omnipresent in the cervigram image, and has a narrow intensity range following the illumination correction step. The mean-standard deviation (mean-std) and the mean-tissue size measured in pixels (mean-size) results were computed over the entire image set for each tissue of the entire data set.



**Table-1.** Tissue statistics averaged over 200 cervigram images.

	SE	CE	AW
MEAN-STD	3.1	5.6	3.8
MEAN-SIZE	754 66	11874	10882

## RESULTS

The Raw cervigram (see Figure-1a) and the converted smoothed intensity gray scale image is shown in Figure-1b. The scaled principle directions overlaid on a map of the normalized principle curvature is also shown in Figure-1c.

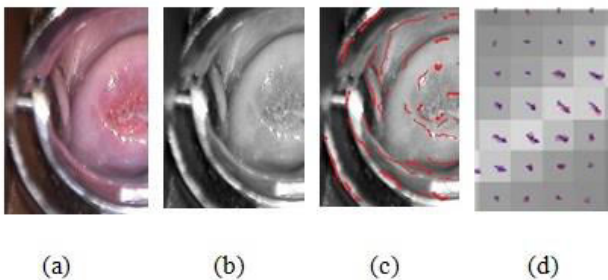


**Figure-1.** Curvature-based boundary indicators. (a) Raw cervigram image (color) (b) Smoothed intensity image (Gray scale) (c) scaled principle directions overlaid on a map of the normalized principle curvature; concave regions-bright; convex regions-dark; (d) Magnified on one of the strong edges in Figure (c).

Here the concave regions are denoted as bright and convex regions as dark. Also one of the strong edges are magnified to see the energy gradient..

## CONCLUSIONS

The raw cervigram acquired by the colposcope is preprocessed by removing the specular reflections and then the region of interest is sought. Before the image is made ready for implementing further image processing algorithms, our novel illumination correction and intensity normalization methods are applied. In the current paper we propose a novel method where we use the polynomial-type Newton's divided difference interpolation for illumination correction. We also find that the squamous epithelial tissue is omnipresent in the cervigram image, and has a narrow intensity range following the illumination correction step. This is based on the observations of mean-standard deviation (mean-std) results that were computed over the entire image set for each tissue of the entire data set. We find that the SE tissue is shown to possess the lowest mean-std value and it occupies most of the cervix region as reflected by the mean-tissue-size measured in pixels. Based on the above observations, we conclude that the peak of the entire cervix region intensity distribution is strongly correlated with the peak of the SE region intensity distribution.

## REFERENCES

- [1] Cancer Facts & Figures 2014, available at: <http://www.cancer.org>.
- [2] D. M. Parkin, F. Bray, J. Ferlay and P. Pisani. 2005. "Global cancer statistics," *Cancer J. Clin.* Vol 55, pp. 74–108.
- [3] P. Basu *et al.* "Evaluation of downstaging in the detection of cervical neoplasia in Kolkata, India," *Int. J. Cancer.* Vol. 100, pp. 92–96.
- [4] R. Sankaranarayanan, R. Rajkumar, R. Theresa, P. O. Esmay, C. Mahe, K. R. Bagyalakshmi, S. Thara, L. Frappart, E. Lucas, R. Muwonge, S. Shanthakumari, D. Jeevan, T. M. Subbarao, D. M. Parkin and J. Cherian. 2004. "Initial results from a randomized trial of cervical visual screening in rural south India," *Int. J. Cancer,* Vol. 109, pp. 461–467.
- [5] L. G. Koss. 1989. "The Papanicolaou test for cervical cancer detection. A triumph and a tragedy," *J. Am. Med. Assoc.* Vol. 261, pp. 737–743.
- [6] S. J. Goldie, L. Gaffikin, J. D Goldhaber-Fiebert, A. Gordillo-Tobar, C. Levin, C. Mahé and T. C. Wright. 2005. "Cost-effectiveness of cervical cancer screening in five developing countries," *N. Engl. J. Med.* Vol 353, pp. 2158–2168.
- [7] Das A. Kar and D. Bhattacharyya. 2011. "Elimination of Specular reflection and Identification of ROI: The First Step in Automated Detection of Uterine Cervical Cancer using Digital Colposcopy" *Proc. of IEEE Imaging Systems & Techniques Penang, Malaysia,* pp. 237-141, doi:1109/IST.2011.5962218
- [8] A.Das, A. Kar and D. Bhattacharyya. 2012. "Implication of Technology on society in Asia: Automated detection of Cervical Cancer" *Proc. of IEEE International Conference on Technology & Society, Singapore.*
- [9] A. Das, A. Kar and D. Bhattacharyya. 2011. "Preprocessing for automatic detection of Cervical Cancer" *Proc. of 15th International Conference on Information Visualisation, London, U.K. ,* ISSN 1550-6037 pp. 597-600, doi: 10.1109/IV.2011.89
- [10] A.Das, A. Kar and D. Bhattacharyya. 2014. "Detection of abnormal regions of pre-cancerous lesions in Digitised Uterine Cervix images" *Proc. of IEEE International Electrical Engineering Congress (iEECON2014), at Pattaya city, Thailand.*
- [11] J. E. Cates, A. E. Lefohn and R. T. Whitaker. 2004. *GIST: an interactive, GPU-based level set*



- segmentation tool for 3D medical images. Vol. 8, No. 3, pp. 217, 2004.
- [12] V. Chalana and Y. Kim. 2002. A methodology for evaluation of boundary detection algorithms on medical images. *IEEE Trans. Medical Imaging*, 16(5):642-652, 1997.
- [13] R. C. Gonzalez and R. E. Woods. 2002. *Digital Image Processing*. Prentice-Hall, Inc.
- [14] S. K. Warfield, M. Kaus, F. A. Jolesz and R. Kikinis. 2000. Adaptive, template moderated, spatially varying statistical classification. *Medical Image Analysis*, Vol. 4, No. 1, pp. 43-55.
- [15] M. Kass, A. Witkin, and D. Terzopoulos. Snakes: active contour models. *International Journal of Computer Vision*, Vol. 1, No. 4, pp. 321-331, 1988.
- [16] S. Osher and J. Sethian. 1998. Fronts propagating with curvature-dependent speed: Algorithms based on the hamilton-jacobi formulation. *Journal of Computational Physics*, Vol. 79, pp. 12-49.
- [17] L. He, Z. Peng, B. Everding, X. Wang, C. Y. Han, K. L. Weiss and W. G. Wee. 2008. Review: A comparative study of deformable contour methods on medical image segmentation. *Image and Vision Computing*, Vol. 26, No. 2, pp.141-163.
- [18] T. Chan and L. Vese. Active contours without edges. *IEEE Trans. Image Processing*, Vol. 10, No. 2, pp. 266-277.
- [19] T. Rohlfing, D. B. Russakoff and C. R. Maurer Jr. 2003. Extraction and application of expert priors to combine multiple segmentations of human brain tissue. In *Proc. of MICCAI*, pp.578-585.
- [20] M. Rousson and N. Paragios. 2002. Shape priors for level set representations. In *Proc. of ECCV*, pp. 78-92.
- [21] Z. Hou. 2006. A review on MR image intensity inhomogeneity correction. *International Journal of Biomedical Imaging*, pp. 1-11.
- [22] T. M. Lehmann and C. Palm. 2001. Color line search for illuminant estimation in real-world scenes. *Optical Society of America*, Vol. 18, No. 11, pp. 2679-2691.
- [23] X. Xie and K. M. Lam. 2005. Face recognition under varying illumination based on a 2d face shape model. *Pattern Recognition*, Vol. 38, pp. 221-230.
- [24] R. Klette, K. Schluns and A. Koschan. 1998. *Computer Vision*. Springer.
- [25] Das, A. Kar and D. Bhattacharyya. 2014. Early Detection of Cervical Cancer using novel segmentation algorithms. *Invertis Journal of Science & Technology*, ISSN 0973-8940, Vol.7 No. 2, pp. 91-95.
- [26] Das A. Kar and D. Bhattacharyya. 2014. Q-Metrics for Early Detection of Cervical Cancer. *Journal of Image Processing & Pattern Recognition Progress*, Vol. 1, pp. 32-36.
- [27] Das, A. Kar and D. Bhattacharyya. Probabilistic Segmentation Methods for Early Detection of Uterine Cervical Cancer. *Journal of Applied Information Science*, ISSN 2321-6115, Vol. 1, pp. 28-31.
- [28] D. J. Jobson, Z. U. Rahman and G. A. Woodell. 1997. A multiscale Retinex for bridging the gap between color images and the human observation of scenes. *IEEE Transactions on Image Processing*, Vol. 6, No. 7, pp. 965-976, July.
- [29] R. Kimmel, M. Elad, D. Shaked, R. Keshet and I. Sobel. 2003. A variational framework for Retinex. *International Journal of Computer Vision*, Vol. 52, No. 1, pp. 7-23.
- [30] Z. Rahman, D. J. Jobson and G. A. Woodell. 2004. Retinex processing for automatic image enhancement. *Journal of Electronic Imaging*, Vol. 13, No. 1, pp. 100-110.
- [31] K. V. Leemput, F. Maes, D. Vandermeulen and P. Suetens. 1999. Automated model based bias field correction of MR images of the brain. *IEEE Trans. on Medical Imaging*, Vol. 18, pp. 885-896, October.
- [32] J. F. Steffensen. *Interpolation*. Chelsea Publishing Company, 1950.
- [33] S. Gordon, S. Lotenberg, R. Long, S. Antani, J. Jeronimo and H. Greenspan. 2009. Evaluation of uterine cervix segmentations using ground truth from multiple experts. *Computerized Medical Imaging and Graphics*, Vol. 33, No. 3, pp. 205-216.
- [34] Carson, S. Belongie, H. Greenspan and J. Malik. *Blobworld*. 2001. Image segmentation using Expectation-Maximization and its application to image querying. *IEEE Trans. on Pattern Analysis and Machine Intelligence*, Vol. 24, No. 8, pp. 1026-1038.